Cytotoxicity of withaferin A in glioblastomas involves induction of an oxidative stress-mediated heat shock response while altering Akt/mTOR and MAPK signaling pathways

Patrick T. Grogan[a,b], **Kristina D. Sleder**[c], **Abbas K. Samadi**[c], **Barbara N. Timmermann**[d], and **Mark S. Cohen**[a,b,*]

[a]Department of Pharmacology, Toxicology, and Therapeutics, University of Kansas Medical Center, Kansas City, Kansas 66160, USA

[b]Department of Surgery, University of Michigan Hospital and Health Systems, Ann Arbor, Michigan 48109, USA

[c]Department of Surgery, University of Kansas Medical Center, Kansas City, Kansas 66160, USA

[d]Department of Medicinal Chemistry, University of Kansas School of Pharmacy, Lawrence, Kansas 66045, USA

Abstract

Withaferin A (WA), a steroidal lactone derived from the plant *Vassobia breviflora*, has been reported to have anti-proliferative, pro-apoptotic, and anti-angiogenic properties against cancer growth. In this study, we identified several key underlying mechanisms of anticancer action of WA in glioblastoma cells. WA was found to inhibit proliferation by inducing a dose-dependent G2/M cell cycle arrest and promoting cell death through both intrinsic and extrinsic apoptotic pathways. This was accompanied by an inhibitory shift in the Akt/mTOR signaling pathway which included diminished expression and/or phosphorylation of Akt, mTOR, p70 S6K, and p85 S6K with increased activation of AMPKα and the tumor suppressor tuberin/TSC2. Alterations in proteins of the MAPK pathway and cell surface receptors like EGFR, Her2/ErbB2, and c-Met were also observed. WA induced an N-acetyl-L-cysteinerepressible enhancement in cellular oxidative potential/stress with subsequent induction of a heat shock stress response primarily through HSP70, HSP32, and HSP27 upregulation and HSF1 downregulation. Taken together, we suggest that WA may represent a promising chemotherapeutic candidate in glioblastoma therapy warranting further translational evaluation.

Keywords

Withaferin A; glioblastoma multiforme; oxidative stress; heat shock response; Akt/mTOR pathway; MAPK pathway

1. Introduction

Malignant gliomas, including the grade IV astrocytoma glioblastoma multiforme (GBM), accounting for 60–70% of such lesions, are the most common adult primary malignant brain

[*]**Corresponding Author:** Mark S. Cohen, MD, FACS, Associate Professor of Surgery, Director of Endocrine Surgery Research, Section of General Surgery, 2920K Taubman Center, SPC 5331, University of Michigan Hospital and Health Systems, 1500 E. Medical Center Drive, Ann Arbor, MI 48109-5331, Telephone: +1 7346154741, Fax: +1 7349365830, cohenmar@med.umich.edu.

tumors, representing approximately 14,000 new cancer cases yearly [1]. The mean post-diagnosis survival time of patients with GBM is approximately 14 months [1; 2]. Most high grade brain tumors are quite infiltrative, resulting in residual invasive tumor cells even after optimal surgical resection. This significantly contributes to the high rate of recurrence and poor clinical outcomes associated with this disease [3]. Standard-of-care management typically involves surgical debulking followed by treatment with radiation and the methylating agent temozolomide. While this currently represents the most efficacious therapy for prolonging survival, tumors are often quick to develop resistance to this line of therapy [4; 5]. Recent investigational therapies have yielded only modest response rates up to 15% at best without impact on 6-month progression-free survival [1; 4].

Therefore, given a lack of current therapeutic strategies to extend survival in glioma patients, there is a critical need for novel therapeutic agents. We previously screened over 200 natural plant extracts with promising anti-tumor potential and identified a 28-carbon steroidal lactone obtained from the *Vassobia breviflora*, withaferin A (WA), with intriguing cytotoxic properties [6]. WA has been identified as a novel cancer therapy with anti-proliferative, proapoptotic, and anti-angiogenic properties as well as a modulator of several key cell-survival and regulatory pathways including those involving Akt, Notch-1, heat shock protein (HSP) 90, NFkappaB, AP-1, estrogen receptor, RET, and p38 among others [7; 8; 9; 10; 11; 12; 13; 14; 15; 16]. Additionally, WA has shown promising anti-tumor activity in several murine xenograft and/or orthograft models including prostate, breast, medullary thyroid, melanoma, uveal melanoma, ovarian, cervical, and brain cancers [15; 17; 18; 19; 20; 21; 22; 23].

We have recently demonstrated the anti-proliferative effects of WA in malignant glioma [24; 25], and this finding was subsequently confirmed demonstrating the thiol-reactivity of WA and its ability to induce a heat shock response via a reporter assay [23]. Several additional reports have identified the pro-oxidant potential of WA [26; 27; 28; 29], however, the mechanism of WA's diverse and widespread effects, especially in glioma cells, is largely unknown. Here, we expand on previous findings to further delineate the nature of WA's anti-cancer effects in glioblastoma and examine the molecular response by the cell.

2. Materials and Methods

2.1 Cell culture and general reagents

Two human glioblastoma multiforme cell lines, U87 and U251, were generously provided by Dr. Jann Sarkaria (Mayo Clinic, Rochester, MN), and one murine GBM cell line, GL26, was graciously donated by Dr. John Ohlfest (University of Minnesota, Minneapolis, MN). All cell lines were grown in Dulbecco's modified Eagle's media (DMEM #6429; Sigma-Aldrich, St. Louis, MO) supplemented with 10% fetal bovine serum (FBS; Sigma- Aldrich, St. Louis, MO) and 1% penicillin/streptomycin (Sigma-Aldrich, St. Louis, MO) at a 37°C humidified atmosphere of 5% CO_2 in air. Withaferin A was extracted and isolated as previously described with a purity of 99% by HPLC and stored as a stock solution, adjusted for impurities, at 20mM in DMSO at −80°C [6]. Propidium iodide (PI), RNase, and N-acetyl-L-cysteine (NAC) were acquired from Sigma-Aldrich (St. Louis, MO), and Annexin VFITC was obtained from BD Biosciences (San Diego, CA).

2.2 Cell proliferation and viability assays

Cells were seeded in 96-well plates at 2,500 cells/well. Following a 6h incubation period, WA-containing media in various concentrations was added to each well, and the cells were incubated for an additional 72h. The number of viable cells was quantified by the colorometric CellTiter96 Aqueous MTS assay (Promega, Fitchburg, WI) at 490nm on a

BioTek Synergy 2 plate reader (BioTek, Winooski, VT) as per the manufacturer's instructions.

Because of the non-enzymatic, auto-reductive potential of NAC, the MTS assay was unable to be utilized for evaluating WA/NAC co-treatment studies given the nature of the assay mechanism, as described by the manufacturer. As such, the CellTiter-Glo luminescent assay (Promega, Fitchburg, WI) was utilized instead to measure cell viability by ATP levels. Cells were plated in 96-well plates followed by treatment with NAC after 6h and WA 1h later. After 72h, assay reagent was prepared as per the instructions, and 50uL was added to each well. The luminescent signal was given 10–20 minutes to equilibrate and quantified by the BioTek Synergy 2 plate reader.

2.3 Cell cycle analysis

Cells were plated at an amount previously determined, based on the growth characteristics of individual cells, to have a high enough yield without achieving complete confluency upon harvest and were allowed to grow overnight. Cells were treated with appropriate concentrations of WA and, where indicated, pre-treated with 5mM NAC. Upon the completion of treatment, cells were trypsinized, collected, resuspended in 0.43mL of 4°C 1x PBS followed by 1mL of −20°C ethanol for a 70% ethanol fixative solution, and stored at −20°C. To analyze, stored cells were collected by centrifugation, resuspended in 1x PBS containing 40ug/mL PI and 100ug/mL RNase, and incubated at −37°C for 30 minutes before being analyzed by flow cytometry (BD LSRII; Becton Dickinson, San Diego, CA). Analysis of these results examined only viable cells without DNA fragmentation to establish the distribution of the true cell cycle in living cells.

2.4 Analysis of cell death

Staining phosphatidylserine on the outer leaflet of the cell membranes on apoptotic cells and DNA staining by PI in necrotic and late apoptotic cells was performed to assess WA-induced cell death. Cells were plated and treated as indicated for cell cycle analysis. Upon the completion of treatment, cells were trypsinized, collected, and washed once in Annexin binding buffer (150mM NaCl, 5mM KCl,1mM $MgCl_2.6H_2O$, 1.8mM $CaCl_2.2H_2O$, 10mM HEPES, and 2% (v/v) FBS). Cells were stained with Annexin V-FITC and PI according to the manufacturer's instructions (BD Biosciences, San Diego, CA) for 20 minutes at 4°C before being washed twice and resuspended in binding buffer. Cells were immediately analyzed by flow cytometry on a BD LSRII.

2.5 Western blotting

Cells were plated and treated in the manner outlined for cell cycle analysis. Proteins were collected, quantified, separated by sodium dodecyl sulfate–polyacrylamide gel electrophoresis (SDS–PAGE), and electrotransfered onto a Hybond nitrocellulose membrane as previously described in Samadi, et al. [30]. Actin levels were assessed to ensure equal loading and transfer of proteins. All studies were repeated for accuracy.

Primary rabbit antibodies against poly(ADP-ribose) polymerase (PARP; #9542; 1:1000), caspase 3 (#9665; 1:1000), caspase 7 (#9492; 1:1000), caspase 9 (#9502; 1:1000), cyclin B_1 (#4138; 1:2000), p-ERK1/2 (Thr202/Tyr204; #4377; 1:1000), Akt (#9272; 1:1000), p-Akt (Ser473; #4058; 1:1000), c-Met (#4560; 1:500), p-c- Met (Tyr1234/1235; #3077; 1:500), epidermal growth factor receptor (EGFR; #4267; 1:1000), p70 S6 kinase (#2708; 1:500), p-p70 S6 kinase (Thr389; #9234; 1:1000), mTOR (#2972; 1:1000), p-mTOR (Ser2448; #2971; 1:1000), Her2/ErbB2 (#2165; 1:1000), 4E-BP1 (#9644; 1:1000); p-4E-BP1 (Thr37/46; #2855; 1:1000), tuberin/TSC2 (#4308; 1:1000), p-tuberin/TSC2 (Thr1462; #3617; 1:1000), AMPKα (#2603; 1:1000), and p-AMPKα (Thr172; #2535; 1:1000) and primary mouse

antibodies against HSP27 (#2402; 1:2000), caspase 8 (#9746; 1:1000), and p-EGFR (Tyr1068; #2236; 1:1000) were acquired from Cell Signaling Technology (Beverly, MA). Total- and phosphoantibodies against p70 S6 kinase were used to detect p85 S6 kinase (phospho-Thr412) given the known crossreactivity of the antibodies. Rabbit antibodies against HSP90 (SPA-836; 1:1000), HSP32/heme oxygenase 1 (SPA- 894; 1:1000), and heat shock factor 1 (HSF1; ADI-SPA-901; 1:1000) were acquired from Enzo Life Sciences (Farmingdale, NY) or its affiliates along with the rat antibody for Grp94 (SPA-850; 1:1000) and the mouse antibody for HSP70 (ADI-SPA-810; 1:1000). The mouse antibody Trap1 (MA1-010; 1:1000) was purchased from Affinity Bioreagents (Pierce Biotechnology, Rockford, IL). A mouse total actin antibody (MAB1501; 1:50,000) to be used as a control was acquired from EMD Millipore (Billerica, MA). A mouse antibody against Raf-1 (sc-7267; 1:250), a goat antibody against p-Raf-1 (Ser338; sc-12358; 1:250), and a rabbit antibody against ERK1/2 (sc-154; 1:5000) were obtained from Santa Cruz Biotechnology (Santa Cruz, CA). Donkey anti-rabbit IgG HRP (sc-2313; 1:5000), goat antimouse IgG HRP (sc-2005; 1:5000), and goat anti-rat IgG HRP (sc-2032; 1:5000) secondary antibodies were also purchased from Santa Cruz Biotechnology. Given primary antibody species specificity, Western analysis was completed in the human U87 and U251 cells lines.

2.6 Detection of ROS

The accumulation of intracellular reactive oxygen species, particularly peroxides like H_2O_2, was determined using CM-H_2DCFDA (Molecular Probes, Grand Island, NY), a general oxidative stress indicator that fluoresces upon oxidation. Cells were preloaded with 20uM CM-H_2DCFDA in 1x dPBS at 37°C for 1h, washed once with phenol redfree DMEM containing 10% FBS and 1% penicillin/streptomycin, and plated in 96-well plates in phenol red-free media at 40,000 cells/well for GL26 and 20,000 cells/well for U87. After 30 minutes, cells were treated with WA, NAC, or both. Measurements were taken on a BioTek Synergy 2 plate reader at 4h with excitation and emission filters of 485nm and 528nm, respectively.

Detection of mitochondrial superoxide present at a given timepoint was examined by MitoSOX Red (Molecular Probes, Grand Island, NY), an indicator reagent that fluoresces upon oxidation by superoxide radicals. Cells were plated and allowed to attach and grow overnight. Pre-treatment with 5mM NAC occurred 1h before treatment with 5uM WA. Cells were harvested 4h after WA addition, washed once with 1x dPBS, and stained with 5uM MitoSOX Red in 1x dPBS for 30 minutes at 37°C. Cells were washed twice with 1x dPBS and run on a BD LSRII flow cytometer (Becton Dickinson, San Diego, CA) with excitation and emission filters of 488nm and 580nm, respectively, to assess mean fluorescence intensity.

2.7 Statistical analysis

GraphPad (GraphPad Inc., San Diego, CA) was used to generate best-fit sigmoidal dose response curves for IC_{50} determination. Comparisons of differences between two or more means were determined by Student's unpaired t-test (2 means) via a standard statistical analysis software package (SPSS version 17.0; SPSS Inc, Chicago, IL). The level of significance was set at $p < 0.05$. Data are presented as mean values with error bars denoting standard deviation. All studies were minimally performed in triplicate unless otherwise noted.

3. Results

3.1 Withaferin A reduces cell proliferation and viability in GBM cells

To investigate the general biological effect of withaferin A in glioblastoma cells, three cell lines (U87, U251, and GL26) were incubated with increasing concentrations of WA or a DMSO control for 72h. Cell number and viability were subsequently determined by using the MTS assay (Fig. 1). WA dose escalation reduced cell proliferation and viability. By GraphPad analysis, the IC_{50} values of WA were determined to be $1.07\pm0.071\mu M$, $0.69\pm0.041\mu M$, and $0.23\pm0.015\mu M$ for U87, U251, and GL26 cells, respectively.

3.2 Withaferin A induces G2/M cell cycle arrest in GBM cells in a dose-dependent manner

In order to establish the nature of the anti-proliferative response to WA, distribution of the cell cycle phases of glioblastoma cells was assessed by flow cytometry at 24h. WA induced a dose-dependent shift in cell cycle arrest from the G0/G1 checkpoint to G2/M arrest. Maximal shift to G2/M arrest above baseline was observed at $0.75\mu M$ in U87 cells (12.0% G2/M in controls increasing to 63.4% with treatment), $1.5\mu M$ in U251 cells (19.1% baseline to 49.7% with treatment), and $0.5\mu M$ in GL26 cells (21.7% baseline to 58.7% with treatment (Fig. 2a). Doses above these optimal levels showed a somewhat diminished G2/M cell cycle shift. The shift to G2/M cell cycle arrest is accompanied by a depletion of cells in the G0/G1 phase and a relative increase in S phase as observed in the U87 (11%) and GL26 (14%), whereas the S phase proportion in U251 cells was largely unchanged (Fig. 2a).

To confirm these findings, the G2/M-specific protein cyclin B_1, which is elevated during G2/M cell cycle arrest, was evaluated by Western blot analysis for increases in expression with WA treatment. At 24h, both U87 and U251 cells demonstrated a dose-dependent induction of cyclin B_1 expression with maximal expression levels observed at $1\mu M$ and $2.5\mu M$ WA, respectively (Fig. 2b). Flow cytometry identified sustained G2/M cell cycle arrest at both 48h and 72h with Western analysis up to 48h supporting those findings (data not shown).

3.3 Withaferin A induces GBM cell death

To further characterize the anti-proliferative effects of WA, annexin V and propidium iodide (PI) dual staining on flow cytometry was used to evaluate the ability of WA to induce cell death through apoptotic and necrotic mechanisms. Fig. 3a illustrates that increases in WA concentration corresponded with enhanced cell death in U87, U251, and GL26 cells at 24h. While all cell lines demonstrated evidence of an apoptotic response indicated by annexin V staining, U87 cells appear to also exhibit increased levels of necrosis with treatment as indicated by staining with PI only. From baseline measurements of 3.9–5.9%, total cell death at $3\mu M$ WA treatment was 51.4% for U87 cells (9.0% early apoptosis; 18.4% late apoptosis; 24.0% necrosis), 24.4% for U251 cells (12.0% early apoptosis; 9.9% late apoptosis; 2.5% necrosis), and 31.7% for GL26 cells (4.4% early apoptosis; 22.2% late apoptosis; 5.1% necrosis). Upon doubling the concentration to $6\mu M$, total cell death increased to 86.9% for U87 cells (3.4% early apoptosis; 55.5% late apoptosis; 28.0% necrosis), 47.1% for U251 cells (9.7% early apoptosis; 32.5% late apoptosis; 4.9% necrosis), and 83.1% for GL26 cells (0.6% early apoptosis; 74.1% late apoptosis; 8.4% necrosis). Further induction of apoptosis was observed at 48h (data not shown).

In order to confirm that these cells were undergoing an apoptotic response, protein levels of mitochondrial/intrinsic procaspase 9, extrinsic procaspase 8, effector procaspases 3 and 7, and downstream PARP cleavage were examined by Western blotting (Fig. 3b). With increasing concentrations of WA, a reduction in the levels of all uncleaved caspases was observed at $5\mu M$ in both U87 and U251 cells at 24h. Procaspases 3, 7, and 8 demonstrated

reduced levels at WA concentrations below 5uM in U87 cells. Finally, PARP cleavage was observed at both 2.5 and 5μM WA in both U87 and U251 cell lines. These data confirm that WA-mediated cytotoxicity at concentrations above IC_{50} is in part due to induction of apoptosis in these GBM cells.

3.4 Withaferin A alters normal protein expression and activation in the Akt/mTOR and MAPK pathways

Given the inhibition of proliferation and induction of cell death observed with WA treatment, several proteins associated with the Akt/mTOR and mitogen-activated protein kinase (MAPK) growth, proliferation, and survival pathways as well as key surface membrane proteins that signal to each pathway, known to be important in glioma and other cancers [1], were screened in U87 and U251 cells for total expression and activation via phosphorylation status at 24h post-treatment (Fig. 4). Total levels of Akt and mTOR were reduced with increasing concentrations of WA. Akt and mTOR phosphorylation were dose-dependently diminished in U87 cells, but only p-mTOR was decreased in U251 cells. Total levels of p70 S6 kinase (downstream of mTOR) and its nuclear isoform p85 S6 kinase were largely unchanged in both cell lines with enhanced downregulation only observed in p85 S6K at 5μM WA in U87 cells. Lowdose WA induced phosphorylation of both proteins, but this was reduced and/or further depleted upon achieving levels of 0.5μM WA and above. Expression of total levels of the translation-repressor 4E-BP1 (also downstream of mTOR) was markedly increased in U87 cells with elevated levels of inhibitory phosphorylation upon increasing WA concentration. In contrast, U251 cells exhibited decreased levels of both total and phosphorylated forms of 4E-BP1 with WA treatment suggesting an overall inhibitory alteration to the Akt/mTOR signaling pathway. Negative regulator of the pathway, AMPKα, was sustained or upregulated in total levels at all WA concentrations tested with the exception of 5μM in U87 cells. Another negative regulator, the tumor suppressor tuberin/TSC2, was sustained in U87 cells and upregulated in U251 cells up to 1μM WA before diminishing at increased concentrations. However, activation of both tuberin/TSC2 and AMPKα via phosphorylation was observed at WA levels as low as 0.1–0.25μM and maintained at higher doses. Peak levels were observed between 0.5–2.5μM in a cell-dependent manner.

Next, the effect of WA on the MAPK cascade was assessed since others have previously implicated WA as an inducer of a MAPK-mediated stress response [6; 12]. In the U87 and U251 cells, total levels of ERK1/2 were unchanged with WA treatment over 24h, but p-ERK1/2 levels were elevated with increasing concentrations of WA up to 2.5μM and then diminished at 5μM (Fig. 4). In contrast to U87 cells, which express both p-ERK1 and p-ERK2 at comparable levels with treatment, p-ERK2 predominates expression with WA treatment of U251 cells. Additionally, total levels of upstream Raf-1 were diminished at 2.5–5μM WA but activation of this protein by phosphorylation of serine 338 was observed in a dose-dependent manner with increasing WA concentrations.

EGFR, Her2/ErbB2, and c-Met are commonly amplified and/or mutated surface proteins in glioblastoma and signal both the MAPK and AKT/mTOR pathways. As such attempts have, previous attempts have been made to therapeutically target these proteins [31; 32; 33; 34; 35]. In both GBM cell lines, total levels of EGFR, Her2/ErbB2, and c-Met were decreased at 24h with increasing WA levels with the exception of c-Met upregulation from 0.25–2.5μM WA (Fig. 4). Phosphorylation of EGFR increased with WA treatment, whereas c-Met phosphorylation was slightly elevated over controls at low WA doses but was downregulated at higher WA concentrations.

3.5 Withaferin A elevates pro-oxidant potential in GBM cells and induces a cellular oxidative stress response

WA-induced apoptosis in several cancer types was recently described as being mediated by reactive oxygen species (ROS) generation [26; 27; 28; 29]. Given the role ROS are known to play in a variety of cancer chemotherapeutic agents [36; 37; 38], we examined whether the oxidation status of glioblastoma cells was altered by WA. The production of peroxide-type radicals with CM-H_2DCFDA and mitochondrial accumulation of superoxide radicals with MitoSOX Red was measured in U87 and GL26 cells at 4h post-WA exposure. GL26 and U87 cell lines demonstrated elevated oxidation status in response to increasing concentrations of WA. Peroxides rose 29.4% in GL26 cells (p=0.01) and 90.5% in U87 cells (p=0.003) compared to controls (Fig. 5a) while mitochondrial superoxide increased 10.9% (p=0.002) and 10.8% (p=0.03) above control at 5μM, respectively (Fig. 5b). In order to determine the nature of this response, cells were simultaneously incubated with 5mM of the thiol antioxidant N-acetyl-Lcysteine (NAC), described as both a redox buffer and ROS scavenger [27; 39]. NAC significantly reduced peroxide generation in WA-treated cells and returned levels to near-baseline in both GL26 cells (p=0.006) and U87 cells (p=0.001). NAC reduced levels of mitochondrial superoxide radicals but failed to do so within statistical significance, and levels remained significantly elevated in U87 cells, despite being reduced compared to WA-alone. Induction of a heat shock response was also recently described in cells via a luminescence reporter assay following WA exposure [23]. Consistent with other models of oxidative stress [40; 41], we observed that WA modulates heat shock protein expression levels at both 24h and 48h in U87 and U251 cells (Fig. 5c). While total levels of HSP90 and its isoforms Trap1 and GRP94 were not consistently or significantly altered with changing WA concentration, HSP70 and HSP32 (heme oxygenase 1) were markedly upregulated while HSF-1 was potently downregulated with increasing WA concentration in both a dose-dependent and time-dependent manner (Fig. 5c and 5d). Dose-dependent reduction of HSF1 corresponded with an increase in the higher molecular weight phosphorylated fraction of the total protein remaining. Moderate induction of HSP27 was observed predominantly at 48h with cell line-dependent diminished expression at 5μM, the highest concentration examined.

3.6 Pre-treatment with a thiol-antioxidant protects GBM cells from the anti-proliferative and cytotoxic effects of withaferin A

To determine if the elevated oxidation state induced by WA is responsible for the apoptotic and anti-proliferative effects observed in vitro, proliferation and apoptosis in the GBM cells were examined in the context of co-treatment with NAC. Consistent with the MTS assay data previously generated, WA was shown to diminish cell viability in a dose dependent manner with the highest potency being demonstrated in GL26 cells. Pre-treatment with 0.5, 1, and 5mM NAC enhanced the resulting cell viability, abrogating the anti-proliferative effects of WA such that with 5mM NAC pretreatment, the anti-proliferative effects of WA were completely eliminated at up to 6uM doses in the U87, U251, and GL26 cell lines (Fig. 6a).

Next, the effects of WA on both cell cycle arrest and apoptosis were evaluated by flow cytometry in the context of NAC pretreatment. As previously described, flow cytometry with WA was performed following 1h pretreatment with NAC in U87, U251, and GL26 cells. Analysis of the cell cycle data revealed that NAC pretreatment was able to completely prevent cell cycle shift to G2/M arrest following 1μM WA treatment at 24h (Fig. 6b). This was supported by a lack of dose-dependent increases in expression of cyclin B_1 by Western analysis at 24h when NAC was used in combination with WA (Fig. 6d). Furthermore, dual staining with PI and Annexin V revealed that NAC pre-treatment completely eliminated all dose-dependent apoptosis and necrosis associated with WA treatment (Fig. 6c). This

observation was then confirmed by a lack of PARP cleavage associated with increasing WA concentration when cells were pre-treated with NAC (Fig. 6d).

Finally, WA-mediated effects on heat shock response were evaluated following pretreatment with 5mM NAC. As shown in Figure 6d, NAC pre-treatment effectively prevented induction of HSP70 and HSP32 at 24h postexposure while limiting depletion of HSF1 following WA treatment.

4. Discussion

Over the past decade, withaferin A has emerged as a promising anti-cancer chemotherapeutic agent. Its effects in cancer cells have been described as anti-proliferative, pro-apoptotic, and anti-angiogenic [7, 8; 9; 10; 11; 12; 13; 14; 15; 16]. To date, however, the detailed mechanism of action of WA in malignant gliomas has not been wellelucidated. The results presented in this study demonstrate for the first time that WA is effectively able to induce a dose-dependent progression of G2/M cell cycle arrest followed by apoptosis-mediated cell death in glioblastoma cells. Reduction in both initiator caspases 8 and 9 suggests that WA can dually activate both extrinsic and intrinsic apoptotic pathways, consistent with previous findings in myeloid leukemia [29]. Such effects appear to be a result of enhanced cellular oxidative stress generated by these compounds which can be completely abrogated by pretreatment with NAC. This oxidative stress with WA treatment also leads to induction of several heat shock proteins associated with cellular stress as well as alteration of the MAPK and Akt/mTOR growth and proliferation pathways including several of their corresponding surface receptors EGFR, Her2/ErbB2, and c-Met.

Pharmacological induction of oxidative stress has emerged as an intriguing means by which to mount an anticancer effect. It is thought that pro-oxidant intervention can alter the redox homeostasis of cancer cells, already stressed by exposure to constitutively high levels of ROS not observed in normal cells, by shifting the balance to a state of cytotoxicity [42; 43]. In fact, many investigational chemotherapeutics with redox potential have recently been explored in preclinical and clinical settings [36; 38]. Such an oxidative stress mechanism has also been demonstrated to effectively induce the proteotoxic stress of protein unfolding/misfolding, resulting in a downstream secondary cytotoxicity that likely preferentially affects these already susceptible cancer cells that may warrant exploration in the WA model [41; 44]. In our experiments, induction of HSP70, HSP32, and HSP27 with WA treatment follows previous models of oxidative stress [40; 41] and lends further credence to the pro-oxidant potential of this drug compound.

HSF1, a transcription factor that plays a major role in the expression of heat shock proteins, has been proposed to be a potentially important target in cancer therapy [45]. While control of HSF1, the major mediator of the observed stress response, has been well-studied, regulation of its stability and turnover remains unclear [46]. As such, it remains unknown if WA directly induces HSF1 degradation or if the resulting decrease in expression is due to some cellular feedback mechanism following its role as a transcription factor to induce heat shock protein expression. Here, we demonstrate that WA may represent a pharmacological means by which to downregulate total HSF1 protein levels.

In contrast to studies with other cancer models, superoxide radicals do not appear to be highly elevated in glioblastoma cells upon WA exposure as measured by MitoSOX Red staining, however peroxide-type radicals are elevated in as detected by CM-H$_2$DCFDA [26; 27]. As noted in Figure 5b, it is unclear if the transient but statistically significant elevation in superoxide detected (11% in both cells lines examined) is physiologically relevant. Given that the majority of oxidants measured are known to be potential downstream products of

superoxide, it is possible that these GBM cells express elevated levels of enzymes like superoxide dismutase, either inherently or as a byproduct of maintenance in cell culture [47; 48].

Our data indicate that the thiol reactivity and/or enhanced oxidation state associated with WA treatment can be fully sequestered by NAC and is likely the main mechanism responsible for the cytotoxic effects generated by WA, however, it remains unknown whether WA directly releases and/or induces ROS or if its thiol-reactive properties shift the normal balance of oxidation by altering the responsible cellular regulation. While WA has previously been demonstrated to bind directly to thiols of certain proteins including HSP90 [9; 23], the specificity of such binding has not yet been fully explored. Given the maintained and sometimes elevated levels of certain proteins and signaling pathways evaluated in this study, we hypothesize that some proteins and pathways in gliomas are more susceptible to the effects of WA, whether through direct binding or secondary effects, resulting in dysfunction and degradation.

Although multiple groups, including ours, have demonstrated the ability of WA to downregulate Akt signaling via its total levels and phosphorylation status in several cancer models [6, 7; 11; 15], no reports describe its effects on other proteins in the Akt/mTOR signaling pathway. In this study, WA shifts the balance of such signaling into an inhibitory state, likely representing a plausible means by which the compound limits growth and proliferation in glioma. Because the tumor suppressor phosphatase and tensin homolog (PTEN) is inactivated by genetic alterations in approximately 60% of glioblastomas, including the cell lines U87 and U251 [49], leading to constitutive activation of the Akt/mTOR pathway, the relevance of targeting this pathway is important [50; 51]. Hyperactivated Akt has been shown to result in uncontrolled cell cycle progression and protection from apoptosis [52]. Decreases in the total and phosphorylated levels of Akt, mTOR, p70 S6 kinase, and p85 S6 kinase as observed here with WA treatment represent direct prevention of the pathway's proliferative effects. In the presence of cellular stress, AMPK suppresses mTOR through phosphorylation of the tumor suppressor tuberin/TSC2 or the mTOR subunit Raptor [53]. It has previously been shown that AMPK activation contributes to apoptosis in glioblastoma cells [54]. Upon WA exposure, glioblastoma cells exhibit activating phosphorylation of both tuberin/TSC2 and the catalytic alpha subunit of AMPK.

The ability of WA to induce phosphorylation of proteins in the MAPK cascade such as ERK1/2 and the isoforms p38 and JNK has been previously demonstrated in several other cancer models [6; 12]. While activation of ERK is generally regarded as a pro-survival attribute and may represent a compensatory mechanism of the cells to stress, it has also been shown as a potential pro-apoptotic signal which may explain its role here. In this study activation of ERK1/2 with WA treatment was observed in the setting of increasing levels of PARP cleavage and caspase activation. WA has previously been demonstrated to induce apoptosis through activation of the p38 MAPK [12], so further exploration of ERK's role in WA-induced cell-death in gliomas is warranted.

This study provides new insight into the potent anti-cancer activity of withaferin A against glioblastomas. The findings presented suggest that the underlying mechanism of WA's antiproliferative, pro-apoptotic, and cell-cycle arresting action are mainly due to its induction of oxidative stress and a stress response by the cells leading to alterations in the expression and signaling of several major pathways, especially the Akt/mTOR proliferative pathway. While this drug has great potential to be a novel therapeutic for the treatment of gliomas, future in vivo studies will determine how these mechanistic effects translate

biologically and the role of WA in clinical applications for patients with glioblastoma multiforme.

Acknowledgments

References

1. Wen PY, Kesari S. Malignant gliomas in adults. N Engl J Med. 2008; 359:492–507. [PubMed: 18669428]

2. Stupp R, Hegi ME, Mason WP, van den Bent MJ, Taphoorn MJ, Janzer RC, Ludwin SK, Allgeier A, Fisher B, Belanger K, Hau P, Brandes AA, Gijtenbeek J, Marosi C, Vecht CJ, Mokhtari K, Wesseling P, Villa S, Eisenhauer E, Gorlia T, Weller M, Lacombe D, Cairncross JG, Mirimanoff RO. Effects of radiotherapy with concomitant and adjuvant temozolomide versus radiotherapy alone on survival in glioblastoma in a randomised phase III study: 5-year analysis of the EORTC-NCIC trial. Lancet Oncol. 2009; 10:459–466. [PubMed: 19269895]

3. Giese A, Bjerkvig R, Berens ME, Westphal M. Cost of migration: invasion of malignant gliomas and implications for treatment. J Clin Oncol. 2003; 21:1624–1636. [PubMed: 12697889]

4. Quick A, Patel D, Hadziahmetovic M, Chakravarti A, Mehta M. Current therapeutic paradigms in glioblastoma. Rev Recent Clin Trials. 2010; 5:14–27. [PubMed: 20205684]

5. Chamberlain MC. Temozolomide: therapeutic limitations in the treatment of adult high-grade gliomas. Expert Rev Neurother. 2010; 10:1537–1544. [PubMed: 20925470]

6. Samadi AK, Tong X, Mukerji R, Zhang H, Timmermann BN, Cohen MS. Withaferin A, a cytotoxic steroid from Vassobia breviflora, induces apoptosis in human head and neck squamous cell carcinoma. J Nat Prod. 2010; 73:1476–1481. [PubMed: 20726569]

7. Oh JH, Kwon TK. Withaferin A inhibits tumor necrosis factor-alpha-induced expression of cell adhesion molecules by inactivation of Akt and NF-kappaB in human pulmonary epithelial cells. Int Immunopharmacol. 2009; 9:614–619. [PubMed: 19236958]

8. Koduru S, Kumar R, Srinivasan S, Evers MB, Damodaran C. Notch-1 inhibition by Withaferin-A: a therapeutic target against colon carcinogenesis. Mol Cancer Ther. 2010; 9:202–210. [PubMed: 20053782]

9. Yu Y, Hamza A, Zhang T, Gu M, Zou P, Newman B, Li Y, Gunatilaka AA, Zhan CG, Sun D. Withaferin A targets heat shock protein 90 in pancreatic cancer cells. Biochem Pharmacol. 2010; 79:542–551. [PubMed: 19769945]

10. Stan SD, Zeng Y, Singh SV. Ayurvedic medicine constituent withaferin a causes G2 and M phase cell cycle arrest in human breast cancer cells. Nutr Cancer. 2008; 60(Suppl 1):51–60. [PubMed: 19003581]

11. Oh JH, Lee TJ, Kim SH, Choi YH, Lee SH, Lee JM, Kim YH, Park JW, Kwon TK. Induction of apoptosis by withaferin A in human leukemia U937 cells through down-regulation of Akt phosphorylation. Apoptosis. 2008; 13:1494–1504. [PubMed: 19002588]

12. Mandal C, Dutta A, Mallick A, Chandra S, Misra L, Sangwan RS. Withaferin A induces apoptosis by activating p38 mitogen-activated protein kinase signaling cascade in leukemic cells of lymphoid and myeloid origin through mitochondrial death cascade. Apoptosis. 2008; 13:1450–1464. [PubMed: 18987975]

13. Mohan R, Hammers HJ, Bargagna-Mohan P, Zhan XH, Herbstritt CJ, Ruiz A, Zhang L, Hanson AD, Conner BP, Rougas J, Pribluda VS. Withaferin A is a potent inhibitor of angiogenesis. Angiogenesis. 2004; 7:115–122. [PubMed: 15516832]

14. Singh D, Aggarwal A, Maurya R, Naik S. Withania somnifera inhibits NF-kappaB and AP-1 transcription factors in human peripheral blood and synovial fluid mononuclear cells. Phytother Res. 2007; 21:905–913. [PubMed: 17562568]

15. Samadi AK, Mukerji R, Shah A, Timmermann BN, Cohen MS. A novel RET inhibitor with potent efficacy against medullary thyroid cancer in vivo. Surgery. 2010; 148:1228–1236. discussion 1236. [PubMed: 21134556]

16. Shah N, Kataria H, Kaul SC, Ishii T, Kaur G, Wadhwa R. Effect of the alcoholic extract of Ashwagandha leaves and its components on proliferation, migration, and differentiation of glioblastoma cells: combinational approach for enhanced differentiation. Cancer Sci. 2009; 100:1740–1747. [PubMed: 19575749]

17. Yang HJ, Shi GQ, Dou QP. The tumor proteasome is a primary target for the natural anticancer compound withaferin a isolated from "Indian Winter Cherry". Mol Pharmacol. 2007; 71:426–437. [PubMed: 17093135]

18. Stan SD, Hahm ER, Warin R, Singh SV. Withaferin A causes FOXO3a- and Bim-dependent apoptosis and inhibits growth of human breast cancer cells in vivo. Cancer Res. 2008; 68:7661–7669. [PubMed: 18794155]

19. Devi PU, Kamath R, Rao BS. Radiosensitization of a mouse melanoma by withaferin A: in vivo studies. Indian J Exp Biol. 2000; 38:432–437. [PubMed: 11272405]

20. Samadi AK, Cohen SM, Mukerji R, Chaguturu V, Zhang X, Timmermann BN, Cohen MS, Person EA. Natural withanolide withaferin A induces apoptosis in uveal melanoma cells by suppression of Akt and c-MET activation. Tumor Biol. 2012; 33:1179–1189.

21. Fong MY, Jin S, Rane M, Singh RK, Gupta R, Kakar SS. Withaferin A Synergizes the Therapeutic Effect of Doxorubicin through ROS-Mediated Autophagy in Ovarian Cancer. PLoS One. 2012; 7:e42265. [PubMed: 22860102]

22. Munagala R, Kausar H, Munjal C, Gupta RC. Withaferin A induces p53-dependent apoptosis by repression of HPV oncogenes and upregulation of tumor suppressor proteins in human cervical cancer cells. Carcinogenesis. 2011; 32:1697–1705. [PubMed: 21859835]

23. Santagata S, Xu YM, Wijeratne EM, Kontnik R, Rooney C, Perley CC, Kwon H, Clardy J, Kesari S, Whitesell L, Lindquist S, Gunatilaka AA. Using the Heat-Shock Response To Discover Anticancer Compounds that Target Protein Homeostasis. ACS Chem Biol. 2012; 7:340–349. [PubMed: 22050377]

24. Grogan, PT.; Samadi, AK.; Cohen, MS. Academic Surgical Congress, Journal of Surgical Research, San Antonio, TX. 2010. A novel cytotoxic agent induced apoptosis in malignant gliomas in vitro; p. 341-342.

25. Grogan, PT.; Sleder, KD.; Stecklein, SR.; Cohen, MS. Academic Surgical Congress, Journal of Surgical Research, Huntington Beach, CA. 2011. Vassobia Breviflora Root-Extract Withaferin A As A Novel Cytotoxic And Synergistic Agent Against Malignant Gliomas; p. 311

26. Hahm ER, Moura MB, Kelley EE, Van Houten B, Shiva S, Singh SV. Withaferin A-Induced Apoptosis in Human Breast Cancer Cells Is Mediated by Reactive Oxygen Species. Plos One. 2011; 6:e23354. [PubMed: 21853114]

27. Mayola E, Gallerne C, Esposti DD, Martel C, Pervaiz S, Larue L, Debuire B, Lemoine A, Brenner C, Lemaire C. Withaferin A induces apoptosis in human melanoma cells through generation of reactive oxygen species and down-regulation of Bcl-2. Apoptosis. 2011; 16:1014–1027. [PubMed: 21710254]

28. Widodo N, Priyandoko D, Shah N, Wadhwa R, Kaul SC. Selective killing of cancer cells by Ashwagandha leaf extract and its component Withanone involves ROS signaling. Plos One. 2010; 5:e13536. [PubMed: 20975835]

29. Malik F, Kumar A, Bhushan S, Khan S, Bhatia A, Suri KA, Qazi GN, Singh J. Reactive oxygen species generation and mitochondrial dysfunction in the apoptotic cell death of human myeloid leukemia HL-60 cells by a dietary compound withaferin A with concomitant protection by N-acetyl cysteine. Apoptosis. 2007; 12:2115–2133. [PubMed: 17874299]

30. Samadi AK, Zhang X, Mukerji R, Donnelly AC, Blagg BS, Cohen MS. A novel C-terminal HSP90 inhibitor KU135 induces apoptosis and cell cycle arrest in melanoma cells. Cancer Lett. 2011; 312:158–167. [PubMed: 21924824]

31. Puputti M, Tynninen O, Sihto H, Blom T, Maenpaa H, Isola J, Paetau A, Joensuu H, Nupponen NN. Amplification of KIT, PDGFRA, VEGFR2, and EGFR in gliomas. Mol Cancer Res. 2006; 4:927–934. [PubMed: 17189383]

32. Wullich B, Muller HW, Fischer U, Zang KD, Meese E. Amplified met gene linked to double minutes in human glioblastoma. Eur J Cancer. 1993; 29A:1991–1995. [PubMed: 8280494]

33. Berezowska S, Schlegel J. Targeting ErbB receptors in high-grade glioma. Curr Pharm Des. 2011; 17:2468–2487. [PubMed: 21827413]

34. Potti A, Forseen SE, Koka VK, Pervez H, Koch M, Fraiman G, Mehdi SA, Levitt R. Determination of HER-2/neu overexpression and clinical predictors of survival in a cohort of 347 patients with primary malignant brain tumors. Cancer Invest. 2004; 22:537–544. [PubMed: 15565811]

35. Guessous F, Zhang Y, diPierro C, Marcinkiewicz L, Sarkaria J, Schiff D, Buchanan S, Abounader R. An orally bioavailable c-Met kinase inhibitor potently inhibits brain tumor malignancy and growth. Anticancer Agents Med Chem. 2010; 10:28–35. [PubMed: 20015006]

36. Tew KD, Townsend DM. Redox platforms in cancer drug discovery and development. Curr Opin Chem Biol. 2011; 15:156–161. [PubMed: 21075043]

37. Antosiewicz J, Ziolkowski W, Kar S, Powolny AA, Singh SV. Role of reactive oxygen intermediates in cellular responses to dietary cancer chemopreventive agents. Planta Med. 2008; 74:1570–1579. [PubMed: 18671201]

38. Wondrak GT. Redox-directed cancer therapeutics: molecular mechanisms and opportunities. Antioxid Redox Signal. 2009; 11:3013–3069. [PubMed: 19496700]

39. Deneke SM. Thiol-based antioxidants. Curr Top Cell Regul. 2000; 36:151–180. [PubMed: 10842751]

40. Ansari N, Khodagholi F, Amini M. 2-Ethoxy-4,5-diphenyl-1,3-oxazine-6-one activates the Nrf2/ HO-1 axis and protects against oxidative stress-induced neuronal death. Eur J Pharmacol. 2011; 658:84–90. [PubMed: 21371450]

41. Qiao S, Lamore SD, Cabello CM, Lesson JL, Munoz-Rodriguez JL, Wondrak GT. Thiostrepton is an inducer of oxidative and proteotoxic stress that impairs viability of human melanoma cells but not primary melanocytes. Biochemical Pharmacology. 2012; 83:12.

42. Laurent A, Nicco C, Chereau C, Goulvestre C, Alexandre J, Alves A, Levy E, Goldwasser F, Panis Y, Soubrane O, Weill B, Batteux F. Controlling tumor growth by modulating endogenous production of reactive oxygen species. Cancer Res. 2005; 65:948–956. [PubMed: 15705895]

43. Cabello CM, Bair WB 3rd, Wondrak GT. Experimental therapeutics: targeting the redox Achilles heel of cancer. Curr Opin Investig Drugs. 2007; 8:1022–1037.

44. Xu W, Trepel J, Neckers L. Ras, ROS and proteotoxic stress: a delicate balance. Cancer Cell. 2011; 20:281–282. [PubMed: 21907917]

45. Au Q, Zhang Y, Barber JR, Ng SC, Zhang B. Identification of inhibitors of HSF1 functional activity by highcontent target-based screening. J Biomol Screen. 2009; 14:1165–1175. [PubMed: 19820069]

46. Hu Y, Mivechi NF. Promotion of heat shock factor Hsf1 degradation via adaptor protein filamin A-interacting protein 1-like (FILIP-1L). J Biol Chem. 2011; 286:31397–31408. [PubMed: 21784850]

47. Evans SM, Judy KD, Dunphy I, Jenkins WT, Hwang WT, Nelson PT, Lustig RA, Jenkins K, Magarelli DP, Hahn SM, Collins RA, Grady MS, Koch CJ. Hypoxia is important in the biology and aggression of human glial brain tumors. Clin Cancer Res. 2004; 10:8177–8184. [PubMed: 15623592]

48. Evans SM, Judy KD, Dunphy I, Jenkins WT, Nelson PT, Collins R, Wileyto EP, Jenkins K, Hahn SM, Stevens CW, Judkins AR, Phillips P, Geoerger B, Koch CJ. Comparative measurements of hypoxia in human brain tumors using needle electrodes and EF5 binding. Cancer Res. 2004; 64:1886–1892. [PubMed: 14996753]

49. Lee JJ, Kim BC, Park MJ, Lee YS, Kim YN, Lee BL, Lee JS. PTEN status switches cell fate between premature senescence and apoptosis in glioma exposed to ionizing radiation. Cell Death Differ. 2011; 18:666–677. [PubMed: 21072054]

50. Koul D. PTEN signaling pathways in glioblastoma. Cancer Biology & Therapy. 2008; 7:1321–1325. [PubMed: 18836294]

51. Lino MM, Merlo A. PI3Kinase signaling in glioblastoma. J Neurooncol. 2011; 103:417–427. [PubMed: 21063898]

52. Nogueira V, Park Y, Chen CC, Xu PZ, Chen ML, Tonic I, Unterman T, Hay N. Akt determines replicative senescence and oxidative or oncogenic premature senescence and sensitizes cells to oxidative apoptosis. Cancer Cell. 2008; 14:458–470. [PubMed: 19061837]

53. Mihaylova MM, Shaw RJ. The AMPK signalling pathway coordinates cell growth, autophagy and metabolism. Nat Cell Biol. 2011; 13:1016–1023. [PubMed: 21892142]

54. Zhang WB, Wang Z, Shu F, Jin YH, Liu HY, Wang QJ, Yang Y. Activation of AMP-activated protein kinase by temozolomide contributes to apoptosis in glioblastoma cells via p53 activation and mTORC1 inhibition. J Biol Chem. 2010; 285:40461–40471. [PubMed: 20880848]
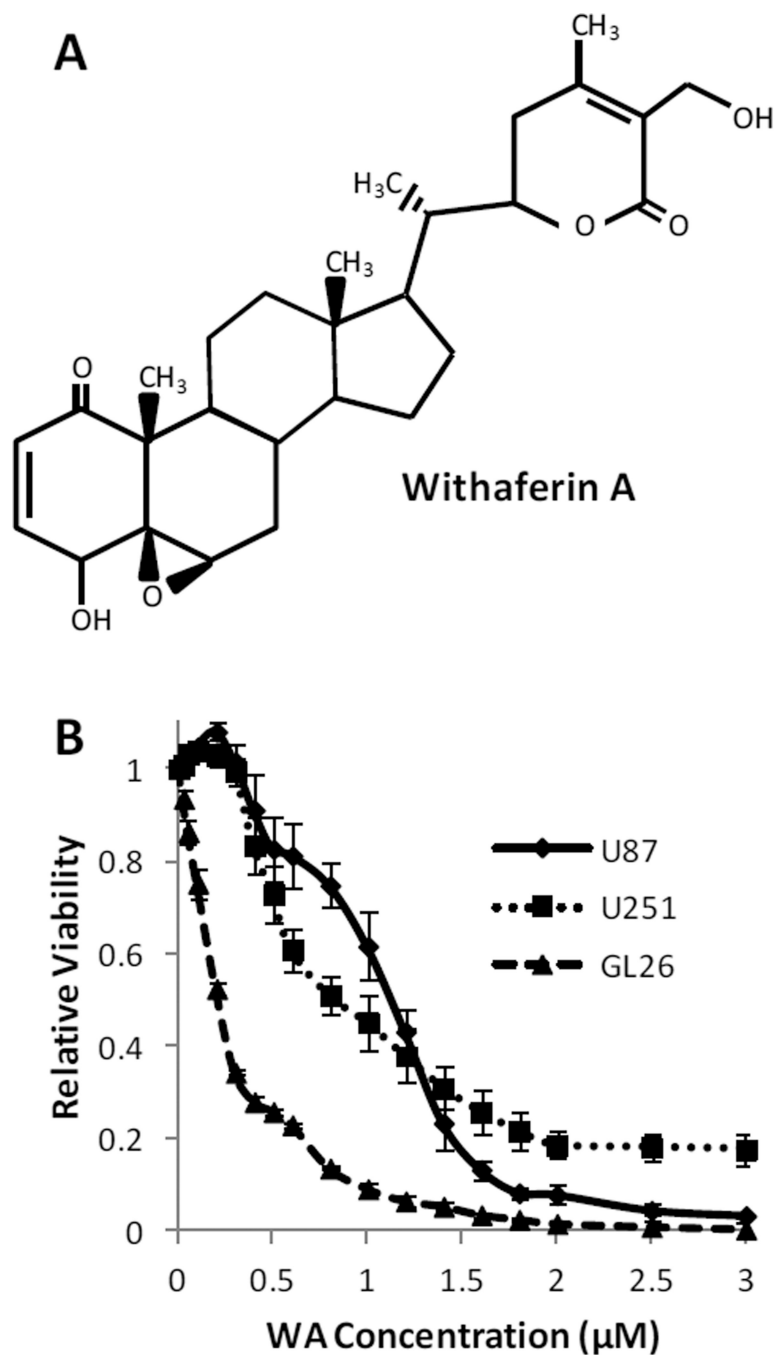
Fig. 1.
(A) Structure of withaferin A. (B) U87, U251, and GL26 cells were incubated with increasing concentrations of WA or a DMSO control for 72h and then assessed by MTS assay. WA dose escalation reduced cell proliferation and viability with IC_{50} values of $1.07\pm0.071\mu M$, $0.69\pm0.041\mu M$, and $0.23\pm0.015\mu M$ for U87, U251, and GL26 cells, respectively
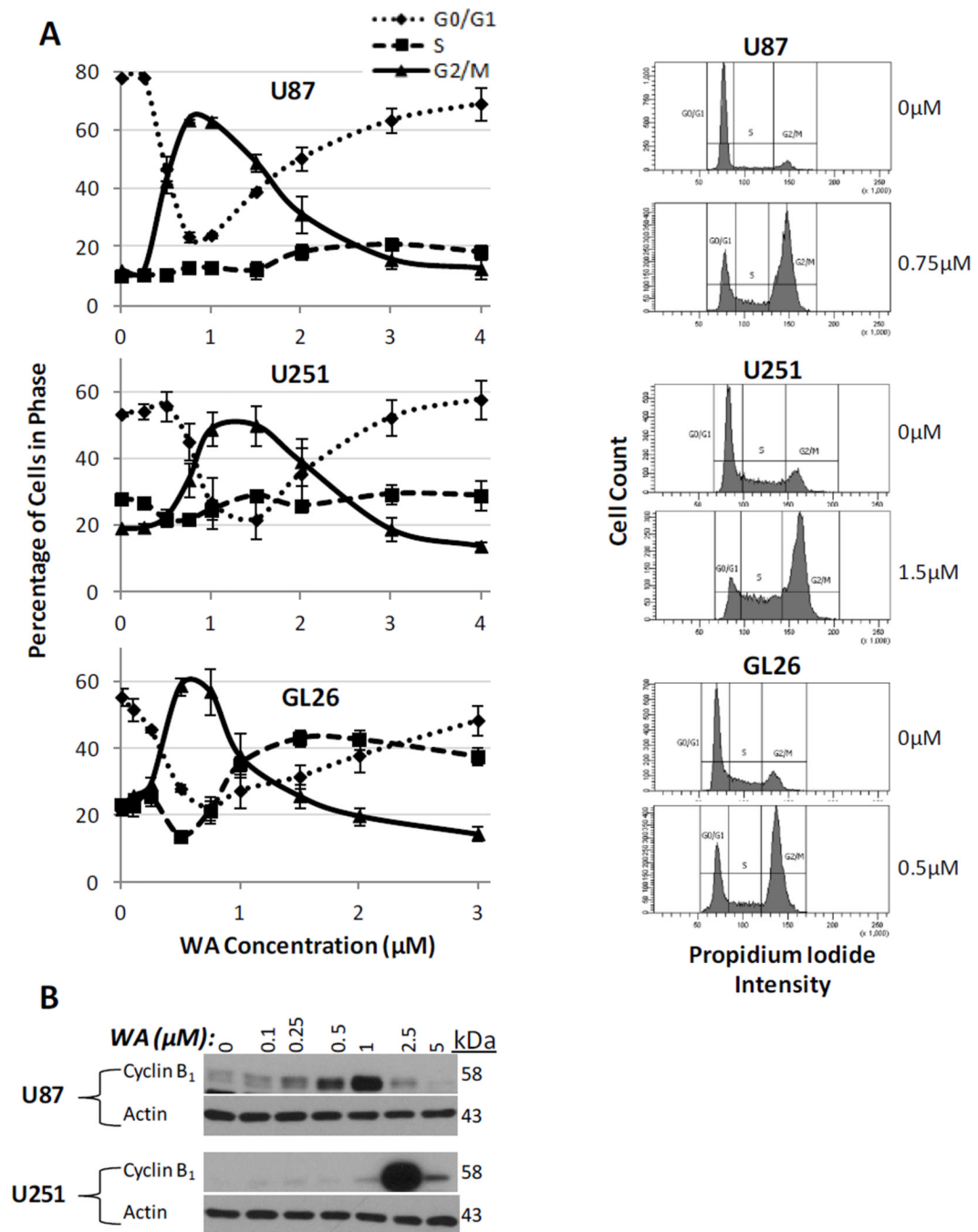
Fig. 2.
(A) Cells stained with propidium iodide and analyzed by flow cytometry revealed that WA induces a dosedependent G2/M cell cycle arrest with an optimal range of such as response at 24h. Maximal induction of arrest above baseline was observed at 0.75μM, 1.5μM, and 0.5μM for U87, U251, and GL26 cells, respectively. Adjacent histograms display representative examples of these peak values in each cell line. (B) G2/M arrest was confirmed by Western blotting for cyclin B_1. At 24h, U87 and U251 cells demonstrated dose-dependent induction of cyclin B_1 with highest levels at 1uM and 2.5μM, respectively
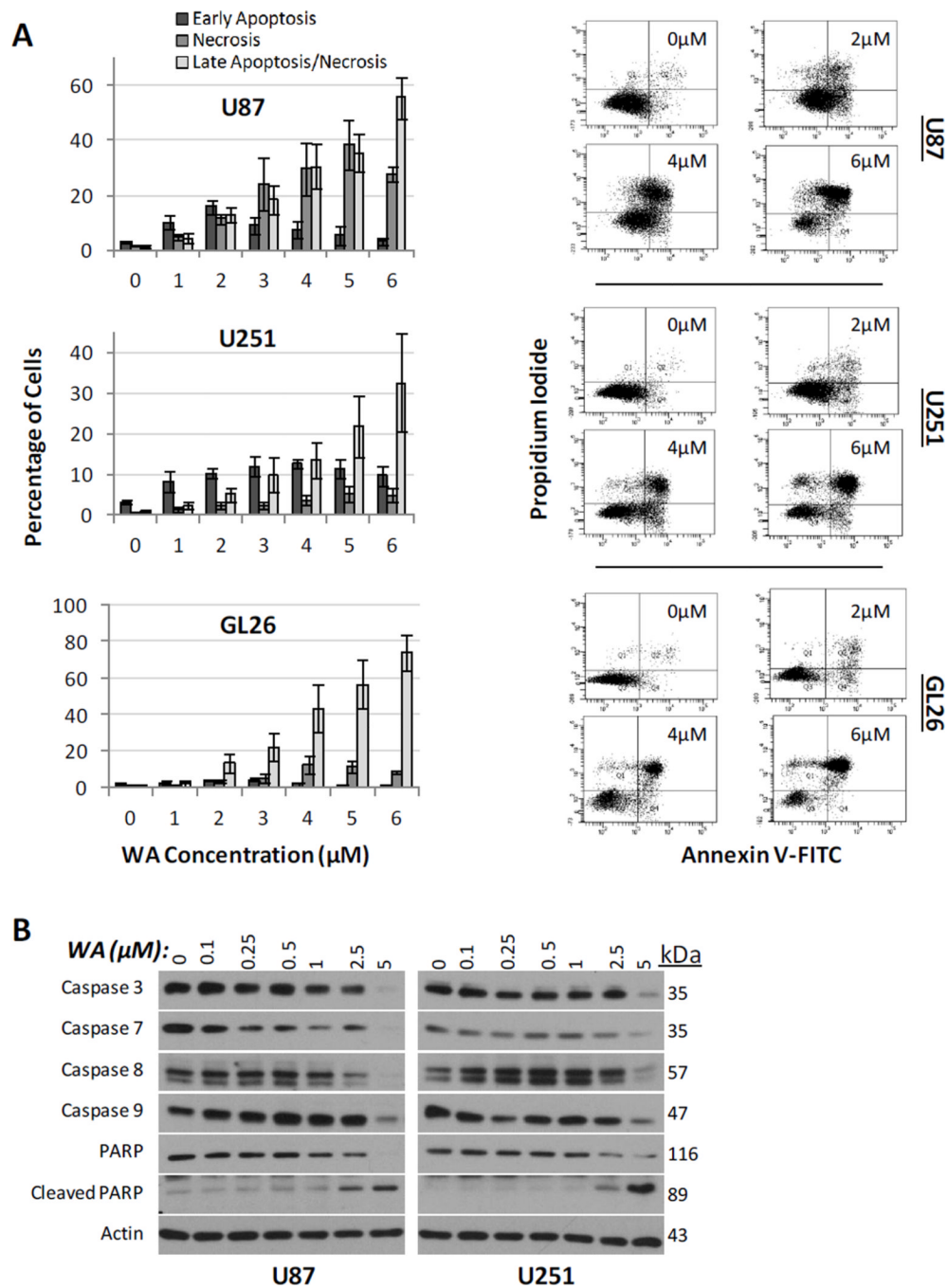
Fig. 3.
(A) Cells stained with propidium iodide and annexin V-FITC and analyzed by flow cytometry revealed that increasing WA concentrations correspond with enhanced cell death in U87, U251, and GL26 cells at 24h. Adjacent dot plots display representative examples of each cell line. (B) Induction of apoptosis was confirmed by Western blotting in U87 and U251 cell lines. WA treatment resulted in reduction in the levels of uncleaved initiator caspases 8 and 9 as well as effector caspases 3 and 7. Further, PARP cleavage was observed at 2.5 and 5µM in both lines
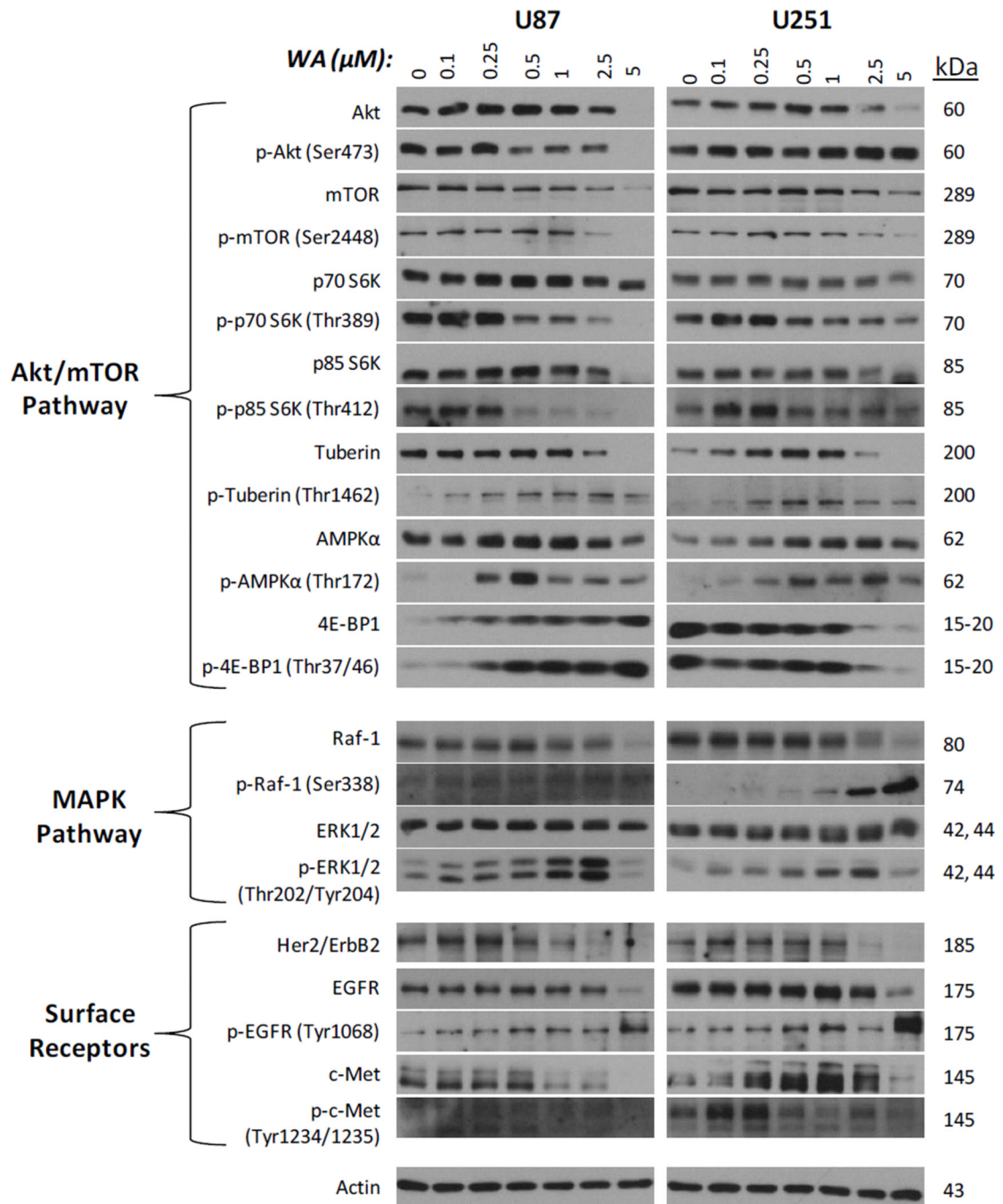
Fig. 4.
Following WA treatment, an array of proteins associated with the Akt/mTOR and MAPK growth, proliferation, and survival pathways as well as surface membrane proteins that signal to each pathway were screened via Western blotting in U87 and U251 cells for total expression and activation via phosphorylation status at 24h post-exposure in order to help evaluate the molecular changes corresponding with cellular observations. Alterations in expression are observed in both pathways and with the cell surface receptors
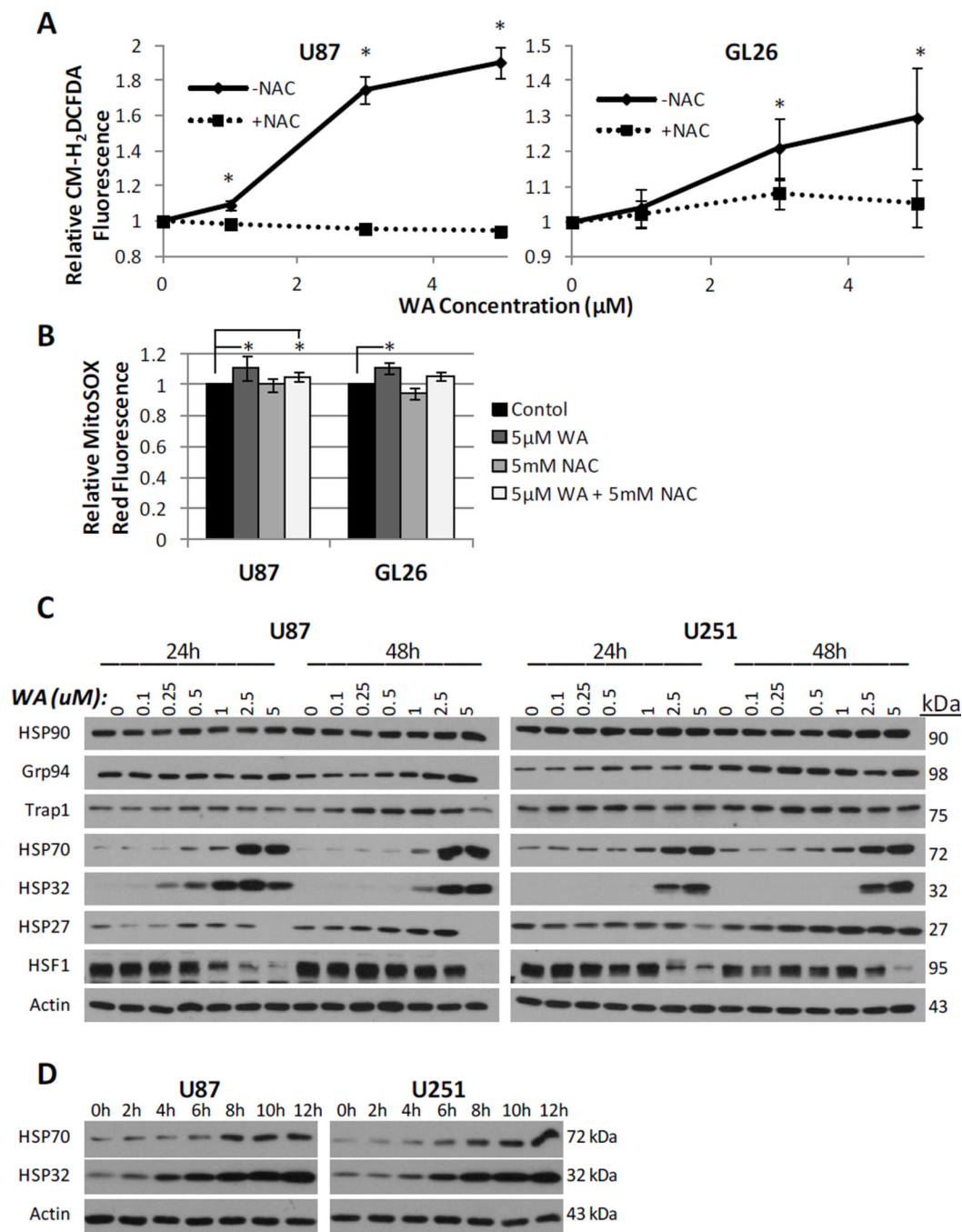
Fig. 5.

(A) Generation of peroxide-type radicals like H_2O_2 following exposure to increasing concentrations of WA were quantified with CM-H_2DCFDA staining in U87 and GL26 cells at 4h. (B) Mitochondrial accumulation of superoxide radicals was assessed by flow cytometry with MitoSOX Red staining in U87 and GL26 cells at 4h post-exposure to 5μM WA. Elevated oxidation status observed in (A) and (B) was reduced or completely eliminated by concurrent treatment with the thiol antioxidant N-acetyl-L-cysteine (5mM). (C) An array of proteins associated with the heat shock stress response were screened via Western blotting in U87 and U251 cells 24h and 48h post-treatment of WA. Upregulation was consistently observed with HSP70 and HSP32 in a dose- and time-dependent manner (C

and D) with alterations in other proteins displaying a cell-specific response. Expression of the transcription factor HSF1 was decreased across both cell lines. *p < 0.05
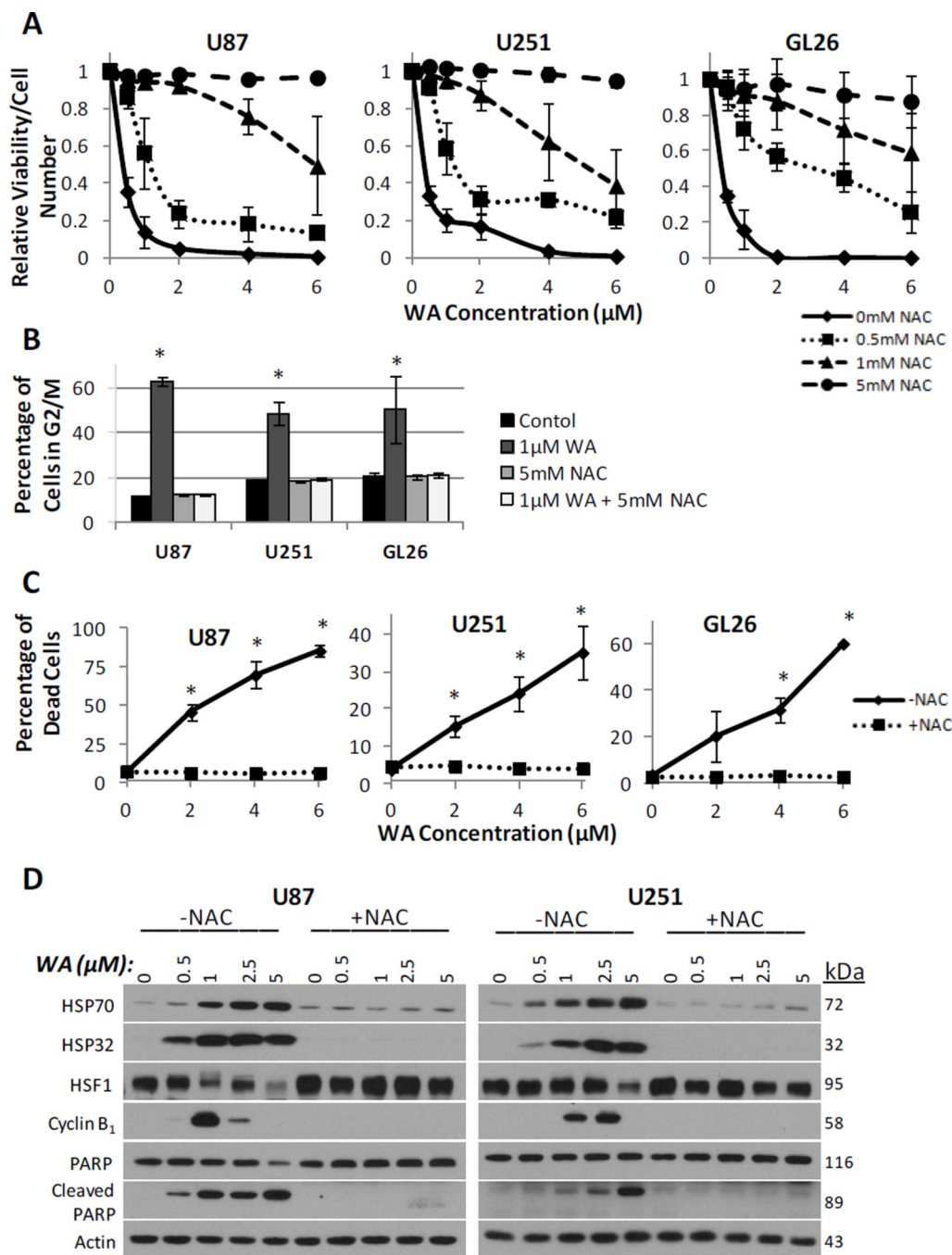
Fig. 6.
N-acetyl-L-cysteine effectively prevented the WA-mediated decrease in viability by the ATP-quantifying CellTiter-Glo assay (A), G2/M cell cycle arrest by propidium iodide staining (B), and cell death by propidium iodide/annexin V-FITC dual staining (C). (D) These findings corresponded with Western analysis for molecular markers of G2/M arrest (cyclin B$_1$) and apoptosis (PARP cleavage) as well as a complete prevention of the heat shock stress response with 5mM NAC pretreatment. *p < 0.05